Molecular Imaging of Proliferation in Malignant Lymphoma

Andreas K. Buck,[1] Martin Bommer,[2] Stephan Stilgenbauer,[2] Malik Juweid,[4] Gerhard Glatting,[1] Holger Schirrmeister,[1] Torsten Mattfeldt,[3] Djurdja Tepsic,[1] Donald Bunjes,[2] Felix M. Mottaghy,[1] Bernd J. Krause,[1] Bernd Neumaier,[1] Hartmut Döhner,[2] Peter Möller,[3] and Sven N. Reske[1]

Departments of [1]Nuclear Medicine and [2]Haematology and [3]Institute of Pathology, University Hospital Ulm, Ulm, Germany and [4]Department of Radiology and the Holden Comprehensive Cancer Center, University of Iowa, Iowa City, Iowa

Abstract

We have determined the ability of positron emission tomography (PET) with the thymidine analogue 3′-deoxy-3′-[^{18}F]fluorothymidine (FLT) to detect manifestation sites of malignant lymphoma, to assess proliferative activity, and to differentiate aggressive from indolent tumors. In this prospective study, FLT-PET was done additionally to routine staging procedures in 34 patients with malignant lymphoma. Sixty minutes after i.v. injection of ~330 MBq FLT, emission and transmission scanning was done. Tracer uptake in lymphoma was evaluated semiquantitatively by calculation of standardized uptake values (SUV) and correlated to tumor grading and proliferation fraction as determined by Ki-67 immunohistochemistry. FLT-PET detected a total of 490 lesions compared with 420 lesions revealed by routine staging. In 11 patients with indolent lymphoma, mean FLT-SUV in biopsied lesions was 2.3 (range, 1.2-4.5). In 21 patients with aggressive lymphoma, a significantly higher FLT uptake was observed (mean FLT-SUV, 5.9; range, 3.2-9.2; $P < 0.0001$) and a cutoff value of SUV = 3 accurately discriminated between indolent and aggressive lymphoma. Linear regression analysis indicated significant correlation of FLT uptake in biopsied lesions and proliferation fraction ($r = 0.84$; $P < 0.0001$). In this clinical study, FLT-PET was suitable for imaging malignant lymphoma and noninvasive assessment of tumor grading. Due to specific imaging of proliferation, FLT may be a superior PET tracer for detection of malignant lymphoma in organs with high physiologic fluorodeoxyglucose uptake and early detection of progression to a more aggressive histology or potential transformation. (Cancer Res 2006; 66(22): 11055-61)

Introduction

Treatment strategies of malignant lymphoma rely on histology and tumor stage. For the last two decades, computed tomography (CT) scanning has been the mainstay diagnostic test for staging of malignant lymphoma and assessment of response to treatment. However, several studies indicated more sensitive lymph node and extranodal staging with positron emission tomography (PET) and the glucose analogue [^{18}F]fluorodeoxyglucose (FDG; refs. 1–3). In aggressive lymphoma, more intense uptake of FDG has been reported compared with indolent lymphoma (4–6). Furthermore, it was shown that persistent FDG uptake in lymphoma after chemotherapy is a strong predictor for early relapse and is superior to conventional CT imaging (7–9). FDG-PET was therefore suggested for assessment of tumor grading and identifying patients needing intensified treatment strategies.

However, FDG is not tumor specific and can also accumulate in inflammatory lesions, such as tuberculosis (granulomas), abscesses, and sarcoidosis (10, 11). Therefore, to increase specificity for malignant lesions, other tracers that complement the information provided by FDG are required. Measurement of tumor growth and DNA synthesis might be appropriate for assessment of proliferative activity in malignant tumors. Several DNA precursors have been investigated thus far, including [^{11}C]thymidine, which represents the native pyrimidine base used for DNA synthesis *in vivo* (12, 13). Due to the short half-life of ^{11}C and rapid degradation of [^{11}C]thymidine, this tracer was considered less suitable for clinical use.

The thymidine analogue 3′-deoxy-3′-[^{18}F]fluorothymidine (FLT), which is derived from the cytostatic drug azidovudine, has been reported to be stable *in vitro* and to accumulate in proliferating tissues and malignant tumors (14). Thymidine kinase 1 (TK1) was revealed as key enzyme responsible for the intracellular trapping of FLT (15, 16). We have shown recently a significant correlation of tumoral proliferation and FLT uptake in a mouse lymphoma xenotransplant model (17) and in human lung cancer (18). Here, we did a prospective study to evaluate whether PET with the novel tracer FLT enables accurate detection of lymphoma and allows assessment of proliferation and tumor grading.

Patients and Methods

This prospective study comprised 34 patients (21 men and 13 women) with a mean age of 51.1 years (range, 19-82 years; Table 1A and B). Patients with histologically confirmed malignant lymphoma who were admitted for pretherapeutic staging (25 patients) or restaging (9 patients) were included. Histopathologic classification was carried out by a hematopathologist (P.M.) in all patients according to the current WHO classification system (19). FLT-PET was done in 12 patients before biopsy and in 22 patients after biopsy. The mean diameter of all biopsied lesions was 32 mm (range, 15-78 mm). Patients who had radiotherapy or chemotherapy within 4 months were excluded from this series. All patients gave written informed consent to participate in the study, which was approved by the local ethical committee.

Immunostaining and evaluation of proliferative activity. In 21 patients, immunostaining of proliferating cells was done additionally to H&E staining. In the remaining patients, respective tissue samples were regarded inappropriate for assessing the proliferation fraction because of the size of tissue sections. The detailed protocol for immunostaining was published elsewhere (18). Briefly, formalin-fixed and paraffin-embedded sections (5 μm) of lymphoma specimens were dewaxed, rehydrated, and microwaved in 0.01 mol/L citrate buffer for 30 minutes. For immunostaining, a monoclonal murine antibody (MIB-1, Dianova, Hamburg, Germany), specific for human nuclear antigen Ki-67, was used (1:500 dilution). Sections

Note: A.K. Buck and M. Bommer contributed equally to this work.

Requests for reprints: Peter Möller, Institute of Pathology, University Hospital Ulm, Robert-Koch-Straβe 8, D-89081 Ulm, Germany. Phone: 49-731-500-23320; Fax: 49-731-500-23321; E-mail: peter.moeller@uniklinik-ulm.de.

doi:10.1158/0008-5472.CAN-06-1955

Table 1. Clinical characteristics, histopathology, and PET-findings in indolent and aggressive lymphoma

A. Correlation of histopathology, FLT/FDG uptake, and proliferation in indolent lymphoma

Patient no.	Histology	Age	Clinical stage	Lesions FLT-PET	Lesions routine staging	Mean FLT-SUV	Mean FDG-SUV	Max FLT-SUV	Max FDG-SUV	Ki-67 index*
2	Follicular lymphoma grade I	60	IV A	79	79	2.1	6.3	3.6	10.2	4
5	Extramedullary plasmacytoma	67	I A	3	3	1.3	2.1	1.8	2.8	n/a
6	Lymphoplasmocytic lymphoma	44	IV A	8	3	2.1	1.4	3.7	1.8	n/a
7	Follicular lymphoma grade I	57	IV B Rel.	53	57	4.5	3.9	8.1	6.1	n/a
9	Follicular lymphoma grade II	70	IV A	5	5	2.9	n/a	4.6	n/a	50
15	Follicular lymphoma NOS	38	IV B Rel.	51	52	2.6	4.5	4.2	6.5	n/a
17	Follicular lymphoma grade I	53	III A	14	14	1.5	3.2	2.7	5.1	1
21	Follicular lymphoma grade I	48	II A E Rel.	3	2	2.7	3.1	4.2	3.9	5
25	Follicular lymphoma grade I	37	III B	29	15	2.8	n/a	5.1	n/a	n/a
28	Follicular lymphoma grade I	53	II A	3	3	1.9	n/a	3.2	n/a	20
31	Extranodal marginal zone lymphoma (MALT type)	58	I E	1	1	1.2	3.2	1.3	3.9	1

B. Correlation of histopathology, FLT/FDG uptake, and proliferation in aggressive lymphoma

1	Diffuse large B-cell lymphoma	70	IV	33	13	5.5	3.1	10.3	4.7	80
3	Diffuse large B-cell lymphoma (anaplastic variant)	44	IV	1	1	4.1	6.6	5.6	10.5	80
8	Diffuse large B-cell lymphoma	64	IV B	6	6	4.8	3.6	5.3	5.5	80
10	Diffuse large B-cell lymphoma (mediastinum)	49	III B Rel.	3	2	4.7	n/a	6.6	n/a	85
11	Diffuse large B-cell lymphoma	43	IV B Rel.	5	5	3.2	3.1	5.6	4.0	n/a
12	Diffuse large B-cell lymphoma (anaplastic variant)	39	IV B	2	2	9.2	n/a	12.3	n/a	n/a
13	Diffuse large B-cell lymphoma	53	III A Rel.	2	2	5.3	n/a	8.7	n/a	80
14	Diffuse large B-cell lymphoma	61	III E Rel.	33	25	5.8	n/a	10.4	n/a	95
16	Diffuse large B-cell lymphoma	56	IV B	11	3	5.7	2.0	9.7	3.2	48
18	Diffuse large B-cell lymphoma	46	I A E	1	1	4.4	5.2	5.9	7.8	n/a
19	Diffuse large B-cell lymphoma (centroblastic variant)	39	IV A E	4	3	8.5	15.9	17.0	21.2	n/a
20	Diffuse large B-cell lymphoma	35	IV B	3	5	3.7	13.2	5.2	22.5	n/a
22	Diffuse large B-cell lymphoma	66	II E B Rel.	59	54	4.8	8.5	8.7	13.8	100
23	Diffuse large B-cell lymphoma (anaplastic variant)	38	III B	17	10	5.8	6.2	9.5	8.3	90
24	Diffuse large B-cell lymphoma (T-cell rich variant)	58	IV B	6	6	6.4	n/a	10.9	n/a	n/a
26	Diffuse large B-cell lymphoma (anaplastic variant)	38	I A	7	3	8.3	n/a	14.3	n/a	90
29	Diffuse large B-cell lymphoma	56	I E Rel.	1	1	3.5	n/a	3.7	n/a	n/a
30	Diffuse large B-cell lymphoma (T-cell rich variant)	64	IV A E	9	8	3.4	n/a	3.7	n/a	80
32	Diffuse large B-cell lymphoma (anaplastic variant)	82	IV A	15	12	8.8	n/a	9.4	n/a	90
33	Diffuse large B-cell lymphoma (anaplastic variant)	50	I B	4	4	8.0	n/a	9.1	n/a	80
34	Diffuse large B-cell lymphoma (NOS)	63	IV E	12	12	5.2	2.1	6.0	2.4	n/a

Abbreviations: Max, maximum; Rel., relapse.
*Number of Ki-67-labeled nuclei per total number of nuclei.

were lightly counterstained with hematoxylin. As positive control for proliferating cells, sections obtained from human normal lymph node tissue (n = 10) were used. The primary antibody was omitted on sections used as negative controls.

MIB-1-stained tissue sections were examined by an experienced pathologist (P.M.) blinded to the results of respective PET scans. Evaluation of MIB-1 immunostaining was carried out in an area with high cellularity as described previously (18). Approximately 800 cells were analyzed per case.

All lymphatic cells with nuclear staining of any intensity were defined as positive. Proliferative activity was described as percentage of MIB-1-stained nuclei per total number of nuclei in the sample.

Synthesis of [^{18}F]FLT, PET imaging, and quantification of lesional FLT uptake. [^{18}F]FLT was produced using the method of Machulla et al. (20) with minor modifications. The detailed synthesis protocol was described elsewhere (21). PET imaging was done using a high-resolution full ring scanner (ECAT Exact or ECAT HR+, Siemens/CTI, Knoxville, TN), which produces 47 or 63 contiguous slices per bed position, respectively. Five bed positions were measured in each patient covering a total field of view of 77.5 cm. The emission scan included the base of the skull, neck, thorax, abdomen, pelvis, and proximal femora in all patients. In 11 patients, the entire skull was included for emission scanning. Patients fasted for at least 6 hours before undergoing PET. Static emission scans were done 60 minutes after injection of 265 to 370 MBq [^{18}F]FLT (mean, 345 MBq). The acquisition time was 10 minutes per bed position. Four-minute transmission scans with a germanium-68/gallium-68 ring source were done for attenuation correction after tracer application. Images were reconstructed using an iterative reconstruction algorithm described by Schmidlin et al. (22).

All images were evaluated by two experienced nuclear medicine physicians (A.K.B. and S.N.R.) without knowledge of the results of histopathologic classification or standard staging procedures. Focal FLT uptake in lymph node basins or organs with usually mild and homogeneous activity were interpreted as manifestation sites of lymphoma. Due to the reduced spatial resolution of PET, no more than three lesions were calculated per single lymph node basin (e.g., the axilla). If both readers produced different results, respective scans were reanalyzed and a consensus was made. Circular regions of interest were drawn containing the area with focally increased FLT uptake to calculate respective standardized uptake values (SUV; FLT-SUV). Mean and maximum values of FLT-SUV were calculated for all lesions and mean values in a reference segment of the lungs, liver, bone marrow, spleen, bone, intestines, and brain.

To estimate the variability of FLT uptake in individual patients, mean and maximum SUVs were calculated in all lesions >20 mm, which were evident at routine clinical staging. In 24 patients, FLT uptake was quantified in a total of 186 lesions. In eight patients with only one or two lesions >20 mm and in two patients with Hodgkin's disease, variability was not assessed.

Routine staging. Routine staging included clinical examination, laboratory screening, chest X-ray, CT of the chest and abdomen, and bone marrow biopsy. Twenty-one patients additionally underwent FDG-PET imaging. FDG uptake in lymphoma lesions was assessed according to the method described for FLT-PET. Additionally, FDG uptake in normal organs was calculated to compare the biodistribution of FLT with that of FDG.

Data analysis. After completion of the study, results of histopathology, immunohistochemistry, routine staging procedures, and FLT-PET findings were compared. Lesions exceeding a number of three in a single lymph node basin were marked as 'multiple' and were not included in the calculation. Data are presented as mean, median, range, and SD. FLT and FDG uptake in indolent and aggressive lymphoma were compared using the Wilcoxon's signed-rank test. Differences were considered significant at a level of $P < 0.05$. For estimation of the variability of tumoral FLT uptake in individual patients, the coefficient of variation (expressed as SD/mean SUV in all lesions) was calculated. The coefficient of variation is a unitless ratio allowing to compare the variability in different patients.

Results

Patients. In 11 patients, histopathology revealed indolent malignant lymphoma (Table 1A), including 6 patients with follicular lymphoma grade I, 1 patient with follicular lymphoma not otherwise specified (NOS), 1 patient with follicular lymphoma grade II, and 1 patient with extranodal marginal zone lymphoma [mucosa-associated lymphoid tissue (MALT) type]. One patient each presented with extramedullary plasmacytoma and lymphoplasmocytic lymphoma, respectively. In 21 patients, aggressive non-Hodgkin's lymphoma was diagnosed (Table 1B). All patients had diffuse large B-cell non-Hodgkin's lymphoma. Two patients with mixed cellularity classic Hodgkin's lymphoma were included in the assessment of FLT uptake (distribution) and proliferative activity but excluded from the statistical analysis comparing indolent with aggressive lymphoma.

Imaging of lymphoma with FLT-PET and FDG-PET. FLT-PET produced images of high contrast of both lymphoma and proliferating tissues (Fig. 1). In all patients, focal FLT uptake could be detected in lymphoma manifestation sites described by routine staging procedures. Preknown manifestation sites were also positive at FDG-PET in 21 patients (sensitivity of FDG-PET, 100%). The specificity of FLT-PET and FDG-PET could not be calculated because all patients had active disease. The total number of lesions in 34 patients was 490 (Table 1A and B). Compared with routine staging procedures (420 lesions), a higher number of lesions were detected on FLT-PET. However, the difference was not statistically

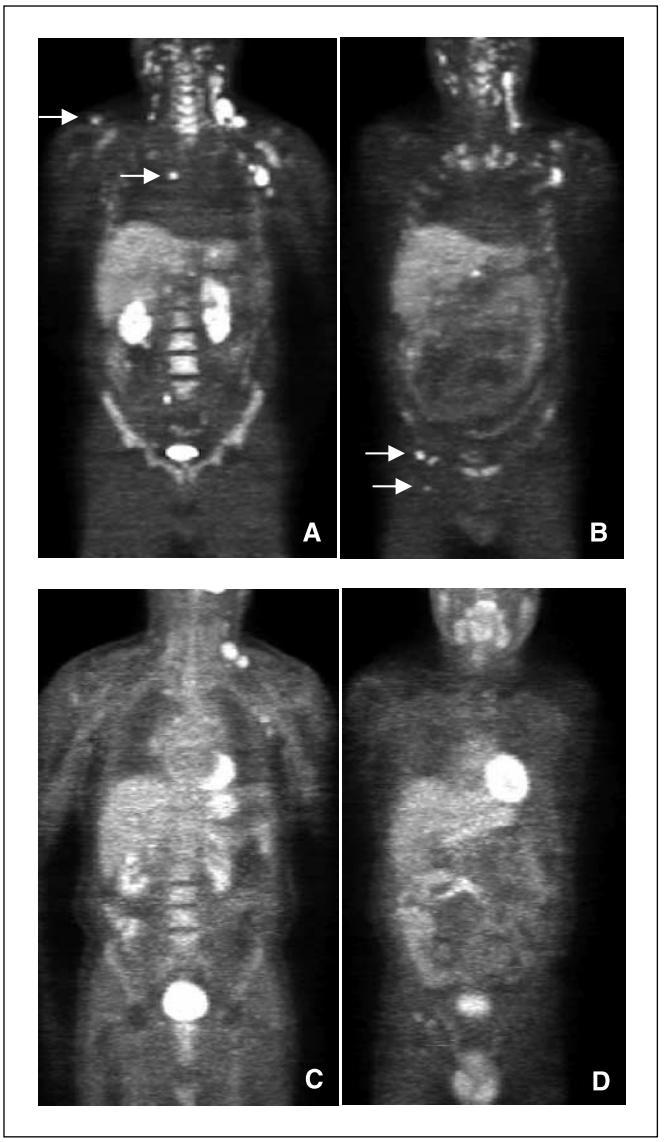

Figure 1. *A* and *B,* coronal sections of FLT-PET in a patient with aggressive lymphoma (patient 1). Intense focal FLT uptake in lymphoma manifestations of the axilla, the neck, the mediastinum, and the right groin. *Arrows,* lesions detected additionally to conventional staging procedures. *C* and *D,* corresponding sections of FDG-PET.

significant (P = 0.23). In 14 patients, a total of 79 additional lesions could be identified (Fig. 1; Table 1A and B). In four patients, the number of detected lesions was lower. Nine lesions were missed in four patients compared with standard staging procedures (Table 1A and B), including three osseous lesions in the vertebral column, which were not detected by FLT-PET. Compared with routine clinical staging, the sensitivity of FLT-PET was 97.8% (411 of 420). However, FLT-PET indicated the same clinical stage in all patients as the standard staging procedures (Table 1A and B).

Biodistribution of FLT. Mean uptake of FLT in lymphoma manifestations was 4.6 (median, 4.7; SD, 2.6; range, 1.2-9.2) and slightly lower compared with respective FDG uptake (mean FDG-SUV, 5.1; median, 4.9; SD, 3.7; range, 1.5-16.2; $P < 0.05$; Fig. 2). Mean maximum FLT uptake in lymphoma was 6.7 (median, 5.7; SD, 3.7; range, 1.3-17.0) and mean maximum uptake of FDG was 8.4 (median, 6.3; SD, 5.9; range, 1.8-22.5; $P < 0.05$). Besides tracer accumulation in malignant lymphoma, high FLT uptake in bone marrow was observed (mean SUV value, 6.9; median, 6.9; range, 3.4-12; Fig. 1). FLT uptake in bone marrow was significantly higher compared with respective uptake in lymphoma ($P < 0.05$). The mean FLT-SUV in a reference segment of the liver was 4.5 (median, 4.3; range, 4.1-6.6), 2.9 in the spleen (median, 1.9; range, 0.8-6.2), 1.9 in the intestines (median, 1.8; range, 0.9-3.4), and 0.5 in the lungs (median, 0.4; range, 0.5-0.9). In the brain, only marginal uptake of FLT was observed (0.2; median, 0.18; range, 0.1-0.8). Figure 2 shows the biodistribution of FLT compared with respective distribution pattern of FDG. Whereas uptake of FLT and FDG in malignant lymphoma was similar, a significantly higher FLT uptake was observed in bone marrow, liver, and spleen ($P < 0.05$; Fig. 3). In patient 22, focal periventricular FLT accumulation indicated cerebral lymphoma manifestation, which was not detected with magnetic resonance imaging (MRI). At follow-up 3 weeks after FLT-PET, cerebral lymphoma was confirmed by MRI and FDG-PET/CT (Fig. 4).

Assessment of tumor grading. Mean FLT uptake (FLT-SUV) in biopsied lesions was 4.5 (median, 4.5; SD, 2.3; range, 1.3-9.2). In 11 patients with indolent lymphoma, the mean FLT uptake in biopsied lesions was 2.3 (median, 2.1; SD, 0.9; range, 1.2-4.5) and the mean maximum FLT was uptake 3.9 (median, 3.7; SD, 1.8; range, 1.3-8.1; Fig. 5; Table 1A). In 21 patients with aggressive lymphoma, the mean FLT uptake was 5.9 (median, 5.5; SD, 1.8; range, 3.2-9.2; Fig. 5; Table 1B) and the mean maximum FLT-SUV was 8.8 (median, 8.7; SD, 3.3; range, 5.0-17.0). Mean FLT-SUV in patients with Hodgkin's lymphoma was 1.7 (maximum FLT-SUV, 2.7). Aggressive lymphoma exhibited a significantly higher FLT uptake compared with indolent lymphoma ($P < 0.0001$; Figs. 3 and 5), and FLT uptake in recurrent disease and primary manifestation sites did not significantly differ (P = 0.76). A cutoff value of SUV = 3 differentiated between indolent and aggressive lymphoma, except for patient 7 with follicular lymphoma grade I and FLT-SUV of 4.5. However, after a 3-week period, the patient was readmitted because of progression of malignant lymphoma. Consecutively, the lymphoma was reclassified as diffuse large B-cell non-Hodgkin's lymphoma, anaplastic variant.

Mean FDG uptake in biopsied lesions was 4.9 (median, 3.6; SD, 3.7; range, 1.4-15.9). In eight patients with indolent lymphoma, the mean FDG uptake in biopsied lesions was 3.5 (median, 3.4; SD, 1.5; range, 1.4-6.3; Table 1A) and the mean maximum FDG uptake was

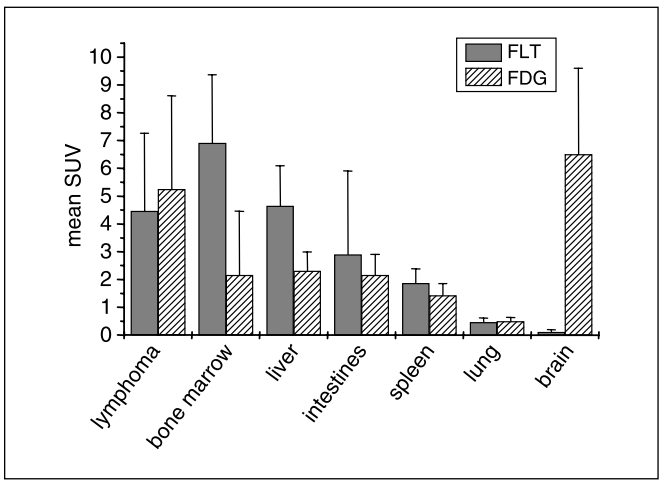

Figure 2. Mean SUV of FLT (FLT-SUV) in malignant lymphoma and reference segments in normal organs (21 patients) compared with respective uptake of the glucose analogue FDG (FDG-SUV).

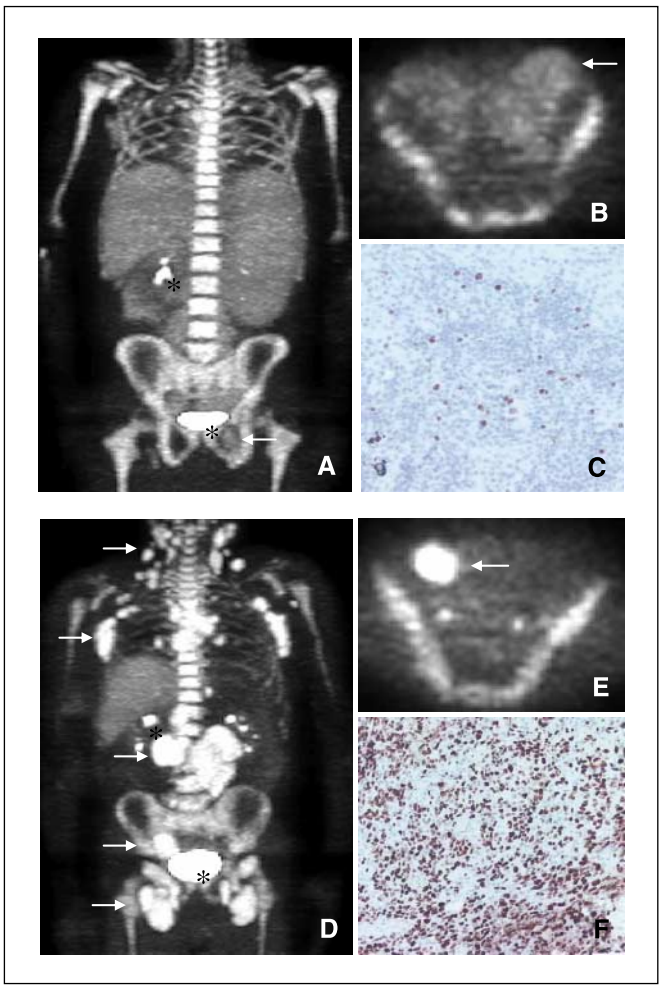

Figure 3. Significantly higher FLT uptake was observed in aggressive compared with indolent lymphoma. *A,* FLT-PET (maximum intensity projection) of patient 2 with indolent lymphoma. Low FLT uptake in an enlarged spleen and in paraaortic, iliac, and inguinal bulky lesions (*arrow*). Physiologic intense FLT uptake in proliferating bone marrow and mild FLT uptake in the liver due to glucoronization of FLT. *B,* transaxial section of the inguinal region, low FLT uptake in lymphoma (*arrow*). *C,* anti-Ki-67 immunostaining (MIB-1) indicates low proliferation fraction of <5%. *D,* FLT-PET (maximum intensity projection) of patient 14 with aggressive lymphoma. Intense uptake of FLT in cervical, axillary, mediastinal, paraaortic, iliac, and inguinal lymph nodes (*arrows*). *E,* transaxial section of inguinal region shows intense FLT uptake in lymphoma (*arrow*). *F,* anti-Ki-67 immunostaining (MIB-1) indicates high proliferation fraction (immunoreactivity in 95% of nuclei).

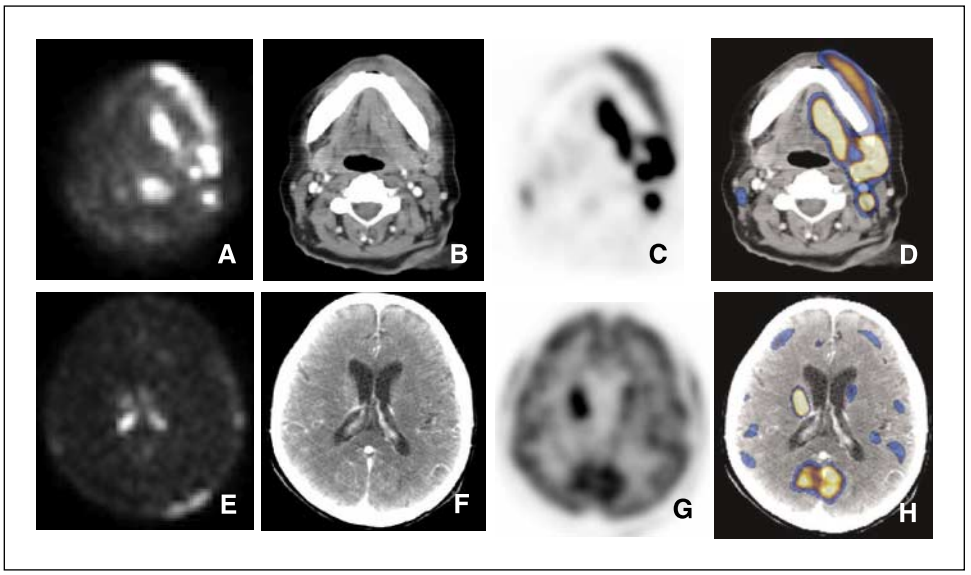

Figure 4. *A,* intense FLT uptake in soft tissue manifestations of aggressive lymphoma and retromandibular lymph nodes (patient 22). Corresponding sections of CT (*B*), FDG-PET (*C*), and FDG-PET/CT image fusion (*D*) at 3-week follow-up show similar location sites of lymphoma. *E,* periventricular FLT uptake indicated cerebral lymphoma manifestation, which was confirmed by CT (*F*), FDG-PET (*G*), and FDG-PET/CT (*H*) at follow-up.

5.1 (median, 4.8; SD, 2.6; range, 1.8-10.2). In 11 patients with aggressive lymphoma, the mean FDG uptake was 6.3 (median, 5.2; SD, 4.6; range, 1.9-15.9; Table 1B) and the mean maximum FDG-SUV was 9.7 (median, 8.1; SD, 6.8; range, 2.2-22.5). Mean FDG-SUV in patients with Hodgkin's lymphoma was 2.5 (maximum FDG-SUV, 4.1). Mean FDG uptake in aggressive lymphoma was not significantly higher compared with indolent lymphoma ($P = 0.17$; Fig. 5). Using maximum FDG-SUV, a significantly higher FDG uptake in aggressive lymphoma was observed ($P < 0.05$).

Using receiver operating characteristic analysis, mean FLT-SUV distinguished between aggressive and indolent lymphoma with an area under the curve (AUC) of 0.98 (maximum FLT-SUV, 0.97), whereas mean FDG-SUV distinguished between these two forms of lymphoma with an AUC of 0.78 (maximum FDG-SUV, 0.79).

Intraindividual variability of FLT uptake. In 15 individual patients with aggressive lymphoma, range of mean FLT-SUV in preknown lesions >20 mm ($n = 113$) was 3.1 to 11.0, and the coefficient of variation ranged from 0.14 to 0.41 (mean value, 0.23). In indolent lymphoma, range of FLT-positive lesions ($n = 73$) was 1.2 to 3.1 in six patients and 0.8 to 8.1 in three patients. The coefficient of variation was 0.21 to 0.43 (mean value, 0.31). Despite considerable variation of FLT-SUV in individual patients, respective SUV values were >3.0 in all patients with aggressive lymphoma. In the majority of indolent lymphoma, FLT-SUV was <3.0. An overlap occurred in three patients with indolent lymphoma presenting with SUV values up to 8.1. Whereas histopathology indicated progression in one of these (patient 7), intense FLT uptake of retroperitoneal lymph nodes could not be verified histologically in two patients (patients 2 and 25, respectively).

Proliferative activity in malignant lymphoma. MIB-1 immunohistochemistry indicated a mean proliferation fraction in lymphoma tissue samples of 61% (median, 50%; SD, 36.1%; range, 1-100%). In indolent lymphoma (6 biopsies), mean proliferation fraction was 13.5% (median, 4.5; SD, 19.2%; range, 1-50%) and in aggressive lymphoma (13 biopsies), mean proliferation fraction was 82.9% (median, 80%; SD, 12.4%; range, 48-100%). Linear regression analysis showed a significant correlation of mean FLT-SUV and Ki-67 index ($r = 0.84$; $P < 0.0001$; Fig. 6*A*). The correlation of mean FDG-SUV and proliferation fraction was not statistically significant ($P = 0.13$; Fig. 6*B*).

Discussion

PET using the glucose analogue 2′-[^{18}F]FDG is now an established imaging modality for staging and restaging of malignant lymphoma (8, 3, 23–25). However, diagnostic accuracy can be reduced by nonspecific uptake of FDG (11). Recently, the thymidine analogue

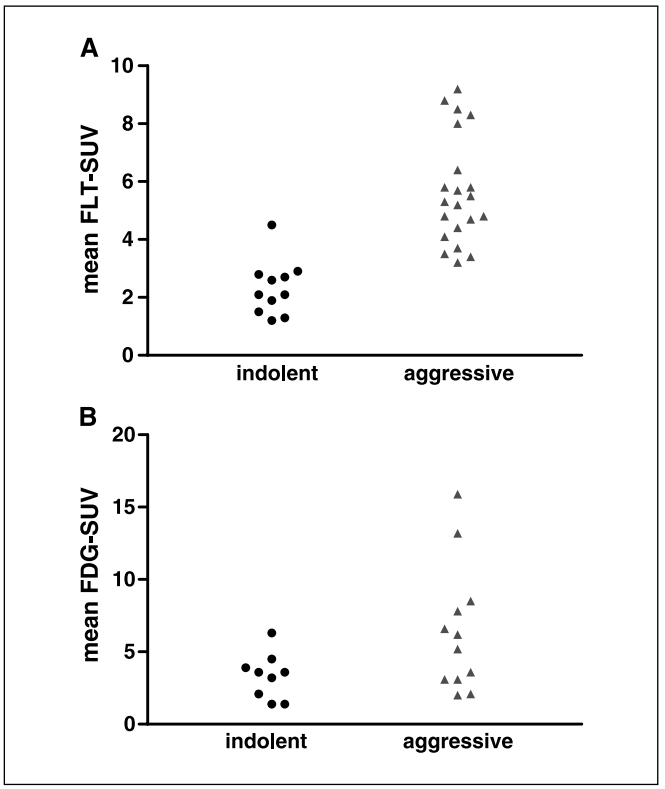

Figure 5. *A,* scattergram of mean FLT-SUV values in biopsied lesions obtained from indolent (11 patients) and aggressive lymphoma (21 patients). Patient 7 with initial diagnosis of indolent lymphoma and high FLT uptake (SUV = 4.5) was reclassified as high-grade lymphoma 3 weeks after PET imaging. Excluding that patient, a cutoff value of SUV = 3 discriminates between indolent and aggressive lymphoma. *B,* mean FDG-SUV values in biopsied lesions from indolent (8 patients) and aggressive lymphoma (11 patients). An overlap of FDG-SUV (1.4-5.8) was observed in indolent and aggressive lymphoma.

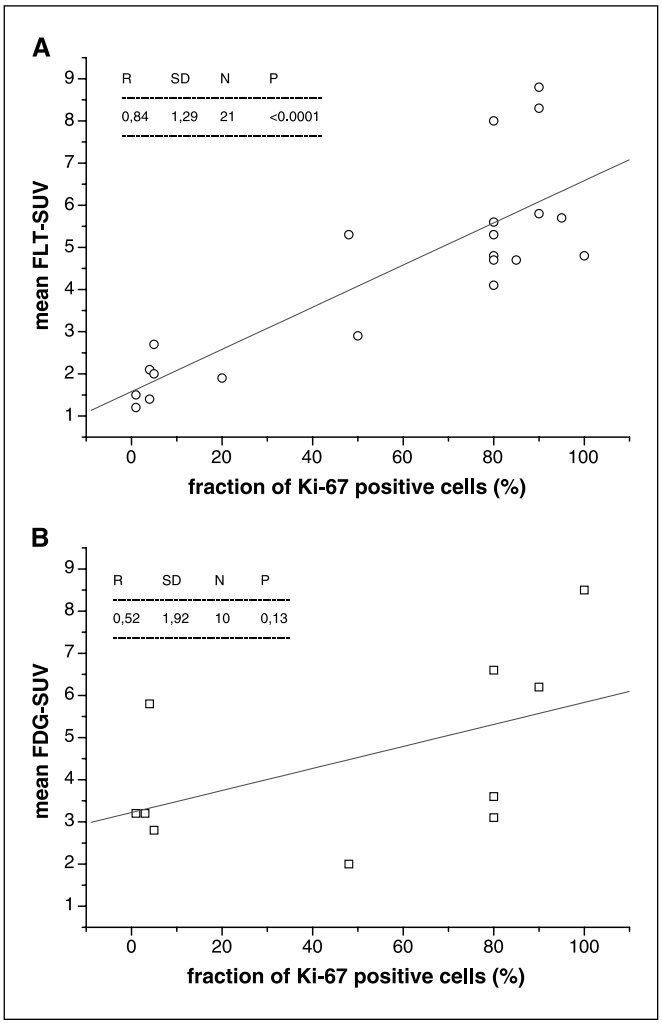

Figure 6. *A,* linear regression analysis shows a significant correlation between FLT uptake in biopsied lesions (mean FLT-SUV) and proliferative activity (Ki-67 index, MIB-1-positive nuclei per total number of nuclei). *B,* linear regression analysis of mean FDG-SUV and proliferative activity (Ki-67 index) was not statistically significant.

3′-deoxy-3′-FLT was suggested for noninvasive assessment of proliferation and more specific tumor imaging (14). In this first clinical trial comprising 34 patients, linear regression analysis indicated a significant correlation of FLT uptake in lymphoma and proliferation fraction in biopsied tissues as indicated by Ki-67 immunohistochemsitry ($r = 0.84$; $P < 0.0001$). A similar correlation of FLT uptake and proliferation fraction was found in solid tumors (18, 26).

However, FLT is not or only marginally incorporated into DNA (<2%) and therefore not a direct measure of proliferation (17, 27). *In vitro* studies indicated that FLT uptake is closely related to TK1 activity and respective protein levels (15, 16). FLT is therefore considered to reflect TK1 activity and, hence, S-phase fraction rather than DNA synthesis.

FLT-PET produced images of high contrast of both lymphoma and proliferating tissues. All patients with indolent or aggressive lymphoma exhibited focal FLT uptake in lesions also described by routine staging procedures. FLT-PET showed additional lesions in 14 patients (Fig. 1) and underestimated extent of disease in 4, indicating a sensitivity of 97.8%. However, staging results according to Ann Arbor classification were the same for FLT-PET and conventional staging procedures. Because of high physiologic tracer uptake in proliferating bone marrow (mean SUV value, 6.9), the sensitivity of FLT for detecting lymphoma manifestations of bone marrow may be reduced. Accordingly, three bone lesions present at routine imaging were not detected. FLT undergoes glucoronization leading to enhanced liver uptake, which was also observed in our series (14). Decreased sensitivity rates were described for liver metastases from various solid tumors (21, 28). In this series, liver manifestations of lymphoma were not observed but may influence diagnostic accuracy of FLT-PET in a larger series. Due to negligible background uptake of FLT in the brain, specific imaging of proliferation may be appropriate for detection of lymphoma in the central nervous system (CNS). In one patient, cerebral manifestation of aggressive lymphoma was indicated by FLT-PET but not MRI (Fig. 4).

A direct comparison of the biodistribution of FLT and FDG was available in 21 patients (Fig. 2). Mean FLT uptake in lymphoma was significantly lower compared with respective FDG uptake. Recently, we observed similar findings in a series of non–small cell lung cancer (21). Whereas sensitivity of FLT-PET was 90% for malignant primaries, detection rates for mediastinal lymph node metastases (53%) and distant metastases (67%) were significantly lower compared with FDG-PET (77% and 100%, respectively) and FLT was interpreted less suitable for tumor staging. In contrast, FLT-PET was accurate for imaging malignant lymphoma in the present series.

An important finding of this study is a significantly higher FLT uptake in aggressive lymphoma compared with indolent lymphoma ($P < 0.0001$; Fig. 5). With the exception of one patient, mean FLT-SUV in biopsied lesions was <3 in patients with indolent lymphoma. Interestingly, this patient was readmitted because of progression and reclassified consecutively as aggressive lymphoma. A high FLT-SUV of 4.5 potentially indicated clinically aggressive and histologically high-grade lymphoma already at initial presentation.

In all other patients with aggressive lymphoma, FLT-SUV was >3 and a cutoff value of FLT-SUV = 3 reliably differentiated between indolent and aggressive lymphoma (Fig. 5). Imaging proliferative activity with FLT-PET seems therefore suitable for noninvasive assessment of tumor grading. These promising results warrant analysis of larger series of patients with more diverse histologic diagnoses.

Semiquantitative evaluation of FDG uptake has also been suggested for differentiation of indolent and aggressive lymphoma (4, 5). Recently, Schoder et al. reported a high likelihood of aggressive lymphoma when respective FDG uptake is >13 (6). An FDG-SUV <6 was highly indicative for indolent lymphoma. However, 45% of the patients remained in a gray zone. A cutoff value of FDG-SUV = 10 would have led to a misclassification rate of 29% in aggressive lymphoma and 19% in indolent lymphomas. In our series, a similar overlap between FDG-SUV of indolent and aggressive lymphoma was observed (Fig. 5). Caution is therefore necessary when SUV values derived from FDG-PET are used for lymphoma grading. Alternatively, calculation of net rate influx of FDG (K_i) from dynamic imaging data and serial blood sampling was suggested for lymphoma grading (4). However, this approach is time consuming and therefore less suitable in a clinical setting. Our data indicate that calculation of SUV values derived from static FLT-PET is accurate for grading of lymphoma.

In daily clinical practice, discrimination between indolent and aggressive lymphoma is based on the percentage of blasts identified in biopsied lesions either by native microscopy and/or by immunostaining of proliferating cells. However, the prognostic value of proliferation fraction as assessed by immunohistochemistry remains a matter of debate. A biopsy is required in all cases

but is suggested to be representative for all lesions only in patients with aggressive lymphoma. In patients with indolent lymphoma, the heterogeneity of lymphoma proliferation can frequently not be identified, except when biopsies from several lymphoma manifestations are done. Therefore, transformation to aggressive lymphoma may be underestimated in some patients. In patients with indolent lymphoma, whole-body FLT-PET may indicate progression in areas with increased FLT uptake and guide biopsy for further verification.

Recently, FLT was suggested for therapeutic monitoring using various experimental settings. In an animal model of fibrosarcoma, it was reported that FLT uptake decreased early after antiproliferative treatment with 5-fluorouracil or cisplatin (29, 30). In a mouse lymphoma xenotransplant model, significant decrease of FLT uptake was observed already 48 hours after chemotherapy with cyclophosphamide (31). However, data are preliminary and clinical trials are needed to further validate FLT as marker for therapy response.

Several limitations have to be taken into account when transferring our results to the clinic. Our findings apply to a particular patient collective, which does not cover all subtypes of malignant lymphoma. Furthermore, SUV values were used to semiquantitatively assess the amount of tracer in tumor manifestations. Uptake in small lesions may be underestimated due to partial volume effects. In the present series, lesions for which SUV calculation has been done had a size larger than 20 mm in all but three patients. In the latter, manifestation sites of lymphoma had a maximum size of 15 mm. All three patients had aggressive disease with an FLT-SUV >4.5, indicating that partial volume effects did not impair the accuracy of FLT-PET. However, partial volume effects may influence the diagnostic accuracy of FLT-PET in a larger series. Calculation of SUV values is therefore recommended only in lesions with a minimum size of 20 mm in diameter, unless correction for partial volume averaging is done. As reported previously for the standard radiotracer FDG, false-positive findings may also occur at FLT-PET because an increased proliferation rate is not specific for malignant tumors. However, false-positive results have not yet been described in the literature.

In conclusion, specific imaging of proliferative activity was as accurate as the standard staging procedures or FDG-PET for staging malignant lymphoma. The use of FLT as PET tracer showed advantages for detection of lymphoma in the CNS and the mediastinum. FLT uptake in lymphoma differentiated between indolent and aggressive lymphoma and indicated progression in one patient. Regions with high proliferation may be identified early in the course of indolent lymphoma leading to more targeted selection of biopsy site and more aggressive therapy.

Acknowledgments

Received 5/30/2006; revised 7/25/2006; accepted 8/31/2006.

Grant support: Deutsche Forschungsgemeinschaft (German Research Foundation) grant Bu-1424/1 (KFO 120, P3) and NIH Lymphoma Specialized Programs of Research Excellence grant (CA 972784) at the University of Iowa.

The costs of publication of this article were defrayed in part by the payment of page charges. This article must therefore be hereby marked *advertisement* in accordance with 18 U.S.C. Section 1734 solely to indicate this fact.

We thank Drs. Brian Link and Sergei Syrbu from the University of Iowa for their critical comments and technical help.

References

1. Moog F, Bangerter M, Diederichs CG, et al. Extranodal malignant lymphoma: detection with FDG PET versus CT. Radiology 1998;206:475–81.
2. Moog F, Bangerter M, Diederichs CG, et al. Lymphoma: role of whole-body 2-deoxy-2-[^{18}F]fluoro-D-glucose (FDG) PET in nodal staging. Radiology 1997; 203:795–800.
3. Jerusalem G, Beguin Y, Fassotte MF, et al. Whole-body positron emission tomography using [^{18}F]fluorodeoxyglucose for posttreatment evaluation in Hodgkin's disease and non-Hodgkin's lymphoma has higher diagnostic and prognostic value than classical computed tomography scan imaging. Blood 1999;94:429–33.
4. Rodriguez M, Rehn S, Ahlstrom H, et al. Predicting malignancy grade with PET in non-Hodgkin's lymphoma. J Nucl Med 1995;36:1790–6.
5. Lapela M, Leskinen S, Minn HR, et al. Increased glucose metabolism in untreated non-Hodgkin's lymphoma: a study with positron emission tomography and fluorine-18-fluorodeoxyglucose. Blood 1995;86:3522–7.
6. Schoder H, Noy A, Gonen M, et al. [^{18}F]Fluorodeoxyglucose uptake in PET distinguishes between indolent and aggressive non-Hodgkin's lymphomas. J Clin Oncol 2005;23:4643–51.
7. Romer W, Hanauske AR, Ziegler S, et al. Positron emission tomography in non-Hodgkin's lymphoma: assessment of chemotherapy with fluorodeoxyglucose. Blood 1998;91:4464–71.
8. Jerusalem G, Beguin Y, Fassotte MF, et al. Early detection of relapse by whole-body positron emission tomography in the follow-up of patients with Hodgkin's disease. Ann Oncol 2003;14:123–30.
9. Spaepen K, Stroobants S, Dupont P, et al. Early restaging positron emission tomography with [^{18}F]fluorodeoxyglucose predicts outcome in patients with aggressive non-Hodgkin's lymphoma. Ann Oncol 2002; 13:1356–63.
10. Kubota R, Kubota K, Yamada S, et al. Microautoradiographic study for the differentiation of intratumoral macrophages, granulation tissues, and cancer cells by the dynamics of fluorine-18-fluorodeoxyglucose uptake. J Nucl Med 1994;35:104–12.
11. Shreve PD, Anzai Y, Wahl RL. Pitfalls in oncologic diagnosis with FDG PET imaging: physiologic and benign variants. Radiographics 1999;19:61–77.
12. Martiat P, Ferrant A, Labar D, et al. *In vivo* measurement of carbon-11 thymidine uptake in non-Hodgkin's lymphoma using positron emission tomography. J Nucl Med 1988;29:1633–7.
13. Wells P, Gunn RN, Alison M, et al. Assessment of proliferation *in vivo* using 2-[^{11}C]thymidine positron emission tomography in advanced intra-abdominal malignancies. Cancer Res 2002;62:5698–702.
14. Shields AF, Grierson JR, Dohmen BM, et al. Imaging proliferation *in vivo* with [^{18}F]FLT and positron emission tomography. Nat Med 1998;4:1334–6.
15. Rasey JS, Grierson JR, Wiens LW, et al. Validation of FLT uptake as a measure of thymidine kinase-1 activity in A549 carcinoma cells. J Nucl Med 2002;43:1210–7.
16. Barthel H, Perumal M, Latigo J, et al. The uptake of 3′-deoxy-3′-[^{18}F]fluorothymidine into L5178Y tumours *in vivo* is dependent on thymidine kinase 1 protein levels. Eur J Nucl Med Mol Imaging 2005;32:257–63.
17. Wagner M, Seitz U, Buck A, et al. 3′-[^{18}F]fluoro-3′-deoxythymidine ([^{18}F]FLT) as positron emission tomography tracer for imaging proliferation in a murine B-cell lymphoma model and in the human disease. Cancer Res 2003;63:2681–7.
18. Buck AK, Schirrmeister H, Hetzel M, et al. 3-Deoxy-3-[^{18}F]fluorothymidine-positron emission tomography for noninvasive assessment of proliferation in pulmonary nodules. Cancer Res 2002;62:3331–4.
19. Jaffe ES, Harris NL, Stein H, et al. Tumours of haematopoietic and lymphoid tissues. Lyon: IARC Press; 2001.
20. Machulla HJ, Blocher A, Kuntzsch M, et al. Simplified labeling approach for synthesizing 3′-deoxy-3′-[^{18}F]fluorothymidine ([^{18}F]FLT). J Radioanal Nucl Chem 2000;24: 843–6.
21. Buck AK, Hetzel M, Schirrmeister H, et al. Clinical relevance of imaging proliferative activity in lung nodules. Eur J Nucl Med Mol Imaging 2005;32:525–33.
22. Schmidlin P. Improved iterative image reconstruction using variable projection binning and abbreviated convolution. Eur J Nucl Med 1994;21:930–6.
23. Wiedmann E, Baican B, Hertel A, et al. Positron emission tomography (PET) for staging and evaluation of response to treatment in patients with Hodgkin's disease. Leuk Lymphoma 1999;34:545–51.
24. Naumann R, Vaic A, Beuthien-Baumann B, et al. Prognostic value of positron emission tomography in the evaluation of post-treatment residual mass in patients with Hodgkin's disease and non-Hodgkin's lymphoma. Br J Haematol 2001;115:793–800.
25. Jerusalem G, Beguin Y, Najjar F, et al. Positron emission tomography (PET) with [^{18}F]fluorodeoxyglucose ([^{18}F]FDG) for the staging of low-grade non-Hodgkin's lymphoma (NHL). Ann Oncol 2001;12:825–30.
26. Vesselle H, Grierson J, Muzi M, et al. *In vivo* validation of 3′deoxy-3′-[^{18}F]fluorothymidine ([^{18}F]FLT) as a proliferation imaging tracer in humans: correlation of [^{18}F]FLT uptake by positron emission tomography with Ki-67 immunohistochemistry and flow cytometry in human lung tumors. Clin Cancer Res 2002;8:3315–23.
27. Lu L, Samuelsson L, Bergstrom M, et al. Rat studies comparing 11C-FMAU, 18F-FLT, and 76Br-BFU as proliferation markers. J Nucl Med 2002;43:1688–98.
28. Francis DL, Visvikis D, Costa DC, et al. Potential impact of [^{18}F]3′-deoxy-3′-fluorothymidine versus [^{18}F]fluoro-2-deoxy-D-glucose in positron emission tomography for colorectal cancer. Eur J Nucl Med Mol Imaging 2003;30:988–94.
29. Barthel H, Cleij MC, Collingridge DR, et al. 3′-Deoxy-3′-[^{18}F]fluorothymidine as a new marker for monitoring tumor response to antiproliferative therapy *in vivo* with positron emission tomography. Cancer Res 2003;63:3791–8.
30. Leyton J, Latigo JR, Perumal M, Dhaliwal H, He Q, Aboagye EO. Early detection of tumor response to chemotherapy by 3′-deoxy-3′-[^{18}F]fluorothymidine positron emission tomography: the effect of cisplatin on a fibrosarcoma tumor model *in vivo*. Cancer Res 2005;65:4202–10.
31. Buck AK, Vogg ATJ, Glatting G, et al. [^{18}F]FLT for monitoring response to antiproliferative therapy in a mouse lymphoma xenotransplant model. J Nucl Med 2004;45:434.

Molecular Imaging of Proliferation in Malignant Lymphoma

Andreas K. Buck, Martin Bommer, Stephan Stilgenbauer, et al.

Cancer Res 2006;66:11055-11061.